PHYSICAL REVIEW A VOLUME 16, NUMBER 3 SEPTEMBER 1977

Mechanism of excitation of two-electron–one-photon K x rays in heavy-ion collisions*†

J. S. Greenberg and P. Vincent
Wright Nuclear Structure Laboratory, Yale University, New Haven, Connecticut 06520

W. Lichten
Becton Center, Yale University, New Haven, Connecticut 06520

(Received 4 March 1977)

The energy dependence of the cross sections for both the $K\alpha$ (one-electron, one-photon) and $K\alpha\alpha$ (two-electron, one-photon) x-ray emissions for Ni-Ni collisions have been measured in the energy range 17.6–91.5 MeV. To account for these observations, we have extended the electron promotion model to the quantitative, *ab initio* calculation of double K-shell vacancies. The results furnish, for the first time, an independent test of both the Briggs-Macek formulation of the electron promotion model and the concept of velocity-dependent exit channels suggested by Fastrup *et al*. We also present, for the first time, a theory of the vacancy-sharing mechanism for double K-shell excitation in symmetric systems. The theoretical results are in quantitative agreement with experiment.

I. INTRODUCTION

Two-electron–one-photon transitions, following inner-shell vacancy production by heavy-ion bombardment, have been reported recently in several ion-atom systems.[1-6] The prominent two-electron transitions to vacant K shells involve two electrons transferred from the L shell ($K\alpha\alpha$), or one electron transferred from both the L and M shells ($K\alpha\beta$). Spectral lines which can be associated with such correlated transitions were also observed at this laboratory in the Ni+Ni system over a range of bombarding energies. Several aspects of these new observations are of particular current interest: (i) The energy of the multielectron transitions, and particularly their transition rates, provide unique information on the deviations from the independent particle description for complex atoms. Especially, as we establish in another publication,[7] the two-electron–one-photon transitions clearly demonstrate that electron correlation effects make contributions to the transition probability which are not only comparable in magnitude to the orbital overlap contributions,[8] but they are crucial in obtaining a physically realistic description of correlated multielectron transitions. (ii) In addition, access to new information on the double K-vacancy production furnishes valuable information on the excitation mechanism which cannot be independently extracted from single vacancy production cross sections. This paper deals with the latter aspects of these studies.

We present measurements of both single and double excitation cross sections as a function of projectile energy. Utilizing the relative cross sections for double and single K-vacancy production as well as the absolute double K-vacancy production probability, these observations furnish, for the first time, an independent test of both the Briggs-Macek[9] formulation of the electron promotion model and the concept of velocity-dependent exit channels, as proposed by Fastrup *et al*.[10] The consideration of the exit channel effect, together with Briggs-Macek mechanism for vacancy production, provides an excellent quantitative framework for interpreting the measurements. We also present, for the first time, a formulation of the vacancy-sharing mechanism[11] for double K-shell excitation in symmetric collision systems.

II. EXPERIMENTAL RESULTS

The experiments were carried out with the MP tandem Van de Graff accelerator of the Wright Nuclear Structure Laboratory, Yale University. Both the projectiles and targets were monoisotopic ^{58}Ni. The targets, consisting of thin (~200 μg/cm^2) nickel foils, were oriented at an angle of 45° to the beam direction. The bombarding energy was varied over a factor greater than 5, with most data accumulated at the four mean projectile interaction energies of 91.5, 64.8, 37.1, and 17.9 MeV. All cross sections were normalized to the accumulated beam charge. The beam was integrated with a Faraday cup which was designed particularly for effective secondary electron emission suppression so that the accumulated charge reflected only the charge of the projectile as predetermined by the magnetic analysis of the beam. A further relative normalization was obtained with a NaI detector viewing the characteristic $K\alpha$ x-ray radiation.

The x-ray spectra were recorded with a 5-mm-thick intrinsic Ge detector, possessing a resolution of ~250 eV at a photon energy of 6 keV. Dur-

TABLE I. Single and double K-shell excitation in collisions of Ni ions with Ni atoms. Comparison of theoretical and experimental results.

Energy (MeV)[d]	17.9	37.1	64.8	91.5
Velocity (a.u.) v	3.48	5.05	6.70	7.94
Cross sections (b) σ_{K_α} (expt)[a]	2510 ± 100	7820 ± 300	17 600 ± 700	30 500 ± 1200
$\omega_K \sigma_{BM}$ (theor)[b] per L-shell vacancy	7800	11 500	16 600	21 300
Exit channel vacancy factor $R = \sigma_{K_\alpha}/\sigma_{BM}\omega_K$	0.32	0.68	1.06	1.43
Vacancy sharing factor $S = (1 + e^{2/v})^{-1}$	0.36	0.402	0.426	0.437
$\sigma_{K_{\alpha\alpha}}$ (expt)[a]	$(1.5 \pm 0.4) \times 10^{-3}$	$(1.2 \pm 0.1) \times 10^{-2}$	$(4.3 \pm 0.3) \times 10^{-2}$	$(1.02 \pm 0.08) \times 10^{-1}$
$\sigma_{K_{\alpha\alpha}}$ (theor)[c] $= \frac{1}{48}\sigma_{BM}\eta S R^2 \omega_{Khs}$	1.1×10^{-3}	0.9×10^{-2}	3×10^{-2}	0.73×10^{-1}

[a] Present results. Only relative errors are given as specified in text.

[b] Scaled from an unpublished calculation of D^+ on D by Briggs and Macek with fluorescent yield from Table IV. We are indebted to R. Laubert for kindly furnishing us with the calculations of the scaled cross sections.

[c] η = branching ratio $= \sigma_{K_{\alpha\alpha}}/\sigma_{Khs} = 1/(5000 \pm 600)$. The velocity dependence of this factor is neglected in this calculation. Source: Ref. 19.

[d] Beam energies (20, 40, 70, and 95 MeV, respectively) were corrected for energy losses to give average energies in the target. See L. C. Northcliffe and R. F. Shilling, Nucl. Data Tables A 7, 233 (1970).

ing the measurement to detect the two-electron, one-photon transitions, an aluminum absorber, 0.034 in. thick, was utilized to suppress the copious $K\alpha$ and $K\beta$ photons so as to reduce the otherwise substantial distortion of the spectral distribution immediately adjacent to these intense spectral lines, and to reduce pileup effects to negligible proportions. To ensure the latter, counting rates were kept below ~50 counts/sec for the total spectrum, and in addition pulse pileup rejection circuitry was employed in independent tests to determine the degree of pulse pileup effects present. All intensities were corrected for absorption effects and detector efficiencies, which were determined with calibrated radioactive sources simulating the geometry of the beam intersection with the target during the experiment. The errors in the absolute cross-section measurements are estimated to include an uncertainty of ±20% in the target thickness in addition to the relative measurement errors given in Table I. The relative errors largely reflect uncertainties associated with the determination of the intensities and spectral distributions of the continuous x-ray backgrounds, errors in extracting peak intensities from a line-shape fitting procedure, uncertain target thickness variations as a function of beam dosage, and statistical errors. The statistical errors contribute a negligible fraction of the total relative error in the $K\alpha$ cross-section measurements, but dominate in the $K\alpha\alpha$ cross-section measurements. It is important to note that the measurements involving only the ratio of signals, such as the slope of the $\sigma_{K\alpha}$ and $\sigma_{K\alpha\alpha}$ variation with projectile energy, as well as the ratio of these two cross sections, are essentially independent of systematic errors such as those associated with the target thickness uncertainty.

The x-ray spectra were accumulated with the x-ray counter positioned both at 90° and 0° to the beam direction. The substantial Doppler shifts (~5% at the projectile energy of 91.5 MeV) of the photon frequencies observed in the 0° data provided an effective separation of the target and projectile related photons. Therefore, for the symmetric collisions studied herein, the observation of this Doppler shift eliminated the possibility that the spectra lines originated from target contaminants. Figure 1 illustrates the relevant regions of the spectra, above the $K\alpha$ and $K\beta$ lines, obtained at four projectile energies for Ni+Ni. In addition to the $K\alpha$, $K\beta$ photons, a prominent line also appears at ~15.3 keV, with a weak transition emerging at ~16.5 keV. Both transitions vary rapidly in intensity and shift in energy with changing projectile energy. As noted above, these lines are not associated with pulse pileup, and, in particular, the observed Doppler shifts at the 0° observation angle verify that they are emitted by Ni atoms and not contaminants in the target. Our analysis of their intensities[7] and energies,[7] as well as concurrent experiments and analyses recently published,[8,12]

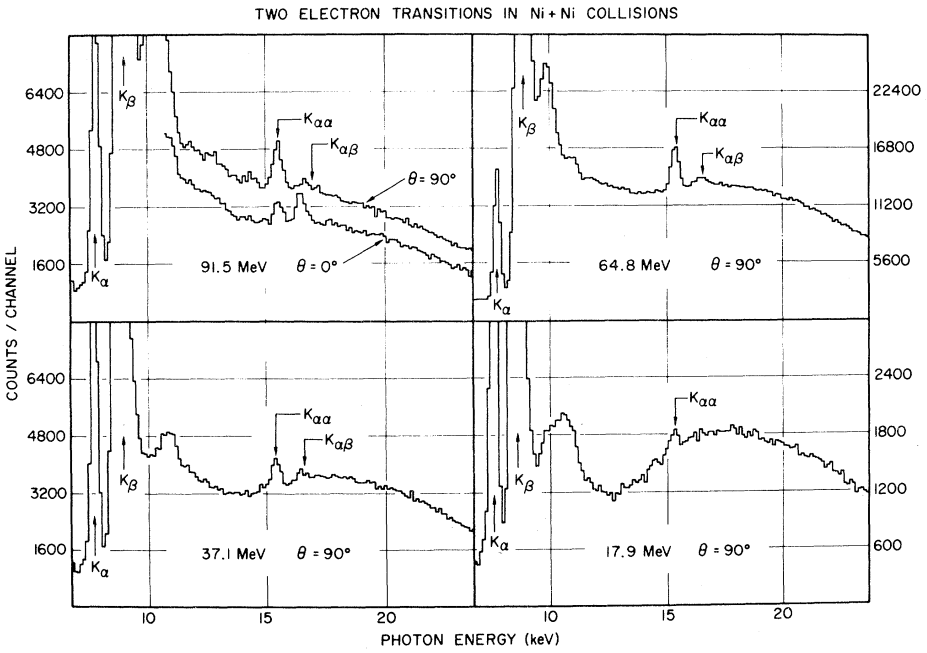

FIG. 1. Observed x-ray spectra of Ni projectiles on Ni targets.

provide convincing proof that these lines can be identified as the $K\alpha\alpha$ and $K\alpha\beta$ two-electron, one-photon transitions which fill a doubly vacant K shell.

Figure 2 displays the total $K\alpha\alpha$ cross sections, as well as the total $K\alpha$ cross sections, derived from these data at the four projectile energies. The ratios of these cross sections are shown in Fig. 3. All experimental errors shown here are statistical only. The total cross sections were obtained from the differential cross sections measured at 90° to the beam direction, assuming isotropic emission. We note that a measurement of the angular distribution of $K\alpha$ x rays at the highest bombarding energies indicated that the 0° and 90° emission anisotropy for this transition was less than 10%.

To systematize the trend, Fig. 2 also compares the cross sections for the $K\alpha$ x ray with a scaled calculation of single vacancy production by Briggs

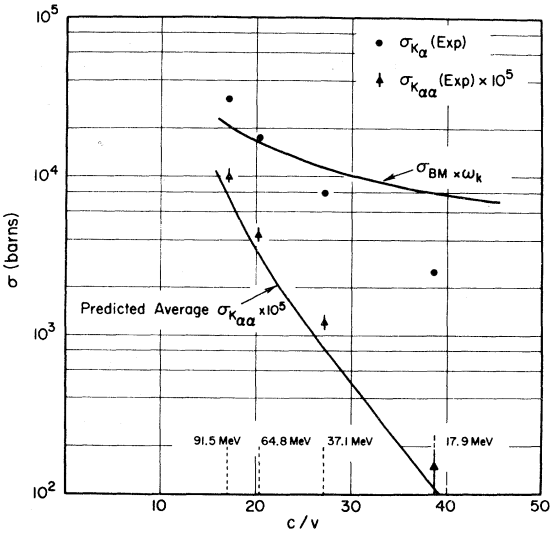

FIG. 2. Comparison of experimental data points with theory.

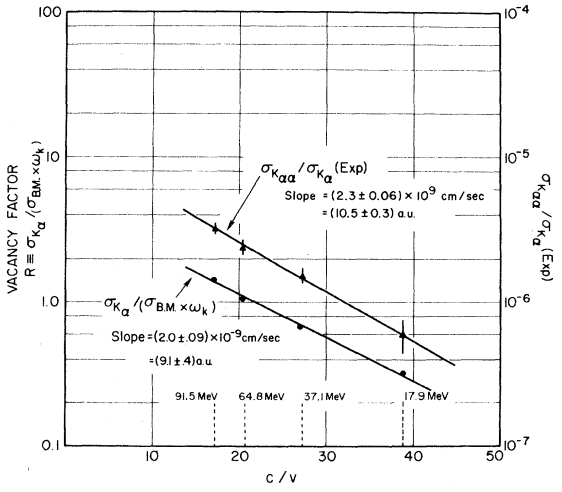

Fig. 3. Test of the dynamically induced exit channels mechanism of Fastrup *et al* . (Ref. 10) and the calculation of Macek and Briggs (Ref. 9), which predict both curves should have the same slope.

and Macek[9] reduced by the neutral atom fluorescence yield factor for nickel of 0.41. The important feature that emerges from this comparison is that the experimental cross section for $K\alpha$ x-ray production is less than the theoretical calculation by a substantial factor at low energies, but exceeds theory at the higher projectile energies.

The plots against the inverse projectile velocity $(1/v)$ emphasize the characteristic exponential falloff of each cross section with $1/v$. As illustrated in the sections that follow, this dominant feature, as well as the absolute slopes and cross sections, can be understood within the framework of the electron promotion mechanism for inner-shell vacancy production[9,13,14] when modified to include dynamic exit channel effects.[10]

III. THEORY

The mechanism of collisional K-shell excitation, in the electron promotion model,[13,14] consists of a rotational coupling of one or both electrons from the $2p\sigma$ molecular orbital (MO) into a vacancy or vacancies in the $2p\pi_x$ MO [process (a) in Fig. 4]. These $2p\sigma$ MO vacancies correlate to K-shell excitation in the separated atoms. Since the probability of a single K-shell excitation is not only proportional to the number of vacancies in the $2p\pi_x$ MO prior to the collision, but also depends on the time evolution of these vacancies, collision induced vacancy production mechanisms can share in importance with the number of $2p\pi_x$ vacancies to be expected[9,14] on the basis of the static electron configuration of the incident projectile. In particular, Fastrup *et al.*[10] have suggested that additional $2p\pi_x$ vacancies can be produced by dynamically induced excitation of $2p\pi_x$ electrons prior to the rotational $2p\sigma$-$2p\pi$ transition [process (b) in Fig. 4]. The dynamic mechanism is velocity dependent, and it is expected to become important at projectile velocities above $0.04\ V_B$[10,15] (V_B is the Bohr velocity of the $1s$ electron in the separated atom). Below this projectile velocity, the predictions of the Briggs-Macek type calculations,[9] based on static vacancy factors alone, have been found to be in quantitative agreement with experiment.[10,15]

This concept of velocity dependent exit channels, as well as the Briggs-Macek[9] formulation of the electron promotion mechanism, can be tested independently with the present experimental cross sections for both single and double K-vacancy production. The Briggs-Macek calculation[9] provides the cross section σ_{BM} for K-shell vacancy production per prior L-shell vacancy. Thus, the ratio R of the K excitation cross section to the value calculated by Briggs and Macek yields the effective number of L-shell vacancies prior to the rotational excitation. The empirically determined vacancy

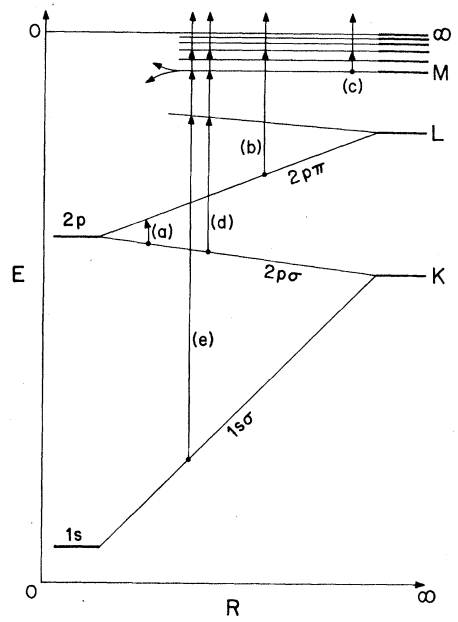

FIG. 4. Excitation mechanisms leading to K-shell excitation in symmetric atomic collisions. See Ref. 36. (a) Rotational $2p\sigma$-$2p\pi$ coupling; (b) excitation out of the $2p\pi$ molecular orbital into outer-shell MO's or to the continuum; (c) excitation of outer-shell MO's; (d) and (e) direct excitation out of the $2p\sigma$ or $1s\sigma$ MO's to outer shells or to the continuum.

factor R can be used to calculate the *double* K-shell vacancy excitation as a function of projectile velocity. In Sec. III B, we show that the probability of a double K-shell excitation is proportional to the *square* of the vacancy factor R.

The Briggs-Macek theory allows for double K-shell excitation. The probability that both excitations end on a single atom is determined in Sec. III C by a readily calculable vacancy sharing probability. An atom with such a double K-shell vacancy can produce the $K\alpha hs$ hypersatellite line[1,12] (a $K\alpha$ line shifted in wavelength) or the much rarer, but more easily resolved, $K\alpha\alpha$ or $K\alpha\beta$ one-photon, two-electron transitions. We note that present measurements provide data within a projectile velocity range (3.48–7.94 a.u., see Table I), from (0.12–0.26) V_B, which is well within the velocity range where dynamic effects are expected to be important.

It is important to note the statistical meaning of the vacancy factor, R. In the original discussion of the exit channels effect,[14] only static vacancies in the electron shells of the incoming projectile were considered. Thus, incoming Ne, Ne^+, and Ne^{++} projectiles were assumed to have 0, 1, and 2 vacancies, respectively, in the p shell. As noted above, Fastrup and co-workers pointed out that this assumption is correct in the low-velocity limit

only.[10] At higher velocities, a velocity-dependent number of dynamically induced vacancies can occur. The *static* number of vacancies is a fixed, definite number. Thus there is no possibility of two K-shell vacancies in a slow, Ne^+-Ne collision where there is one initial L-shell vacancy. On the other hand, the number of *dynamically* induced vacancies is statistical, and there is always a possibility of two vacancies.

In the case under consideration involving Ni projectiles on Ni targets, there are no static L-shell vacancies. All the vacancies are dynamically induced, and are statistical in nature. Even if the vacancy factor R is less than unity, there is still a finite probability of a double vacancy in the L shells of the colliding partners, which can lead to a double K-shell vacancy after the collision. This conclusion holds also in the case of "two-step processes," where the incoming projectile has inner-shell vacancies from a prior collision in the solid target.[16]

We proceed by calculating the single and double K-shell excitation probabilities and cross sections within the framework of the Briggs-Macek calculation, and express the results in terms of the empirically determined vacancy factor R. A consideration of the vacancy sharing mechanism for double K-shell excitation in symmetric collisions then leads to a cross section for double K-vacancy production in either of the separated atoms. $K\alpha\alpha$ x-ray production cross sections are obtained by evaluating the fluorescent yield dependence on the state of L-shell ionization.

A. Single K-vacancy excitations

There are a total of 12 $2p$ atomic orbitals in the separated atoms (SA). These become 12 molecular orbitals in the colliding system. The probability p that any given one of these 12 L-shell MO's is vacant is given by

$$p = \tfrac{1}{12}R \,. \tag{1}$$

The probabilities that the $2p\pi_x$ doubly degenerate MO (the one which leads to K-shell vacancies in the electron promotion model) has a value p_0 of having no vacancies, p_1 of having a single vacancy, and p_2 of having a double vacancy, are given, respectively, by

$$p_0 = (1-p)^2 \,, \tag{2}$$

$$p_1 = 2p(1-p) \,, \tag{3}$$

and

$$p_2 = p^2 \,. \tag{4}$$

Therefore, the mean number of $p\pi_x$ vacancies is $p_1 + 2p_2 = 2p = \frac{1}{6}R$.

A measure of the relative magnitudes of these probabilities is obtained by considering, on the average, one p-shell vacancy prior to the collision. The vacancy factor then becomes unity ($R = 1$), and the p-shell vacancy probability, as given by expression (1), is $p = \frac{1}{12}R = \frac{1}{12}$. The probabilities of zero, one, and two $p\pi_x$ vacancies, respectively, are

$$p_0 = (1-p)^2 = (\tfrac{11}{12})^2 = \tfrac{121}{144} \,,$$

$$p_1 = 2p(1-p) = 2 \times \tfrac{1}{12} \times \tfrac{11}{12} = \tfrac{22}{144} \,,$$

and

$$p_2 = p^2 = (\tfrac{1}{12})^2 = \tfrac{1}{144} \,,$$

and the expectation value for the total number of vacancies is $p_1 + 2p_2 = \frac{1}{6}$. It is particularly significant to note the small, but nonzero, probability of a double vacancy with a vacancy factor of unity.

Briggs and Macek calculated the total cross section for K-shell excitation to be given by the expression[9]

$$\begin{aligned}\sigma(K) &= \sigma(2p\sigma^{-1}) \\ &= 2\pi \int_0^\infty \{p_1 P(b) + 2p_2 P(b) \\ &\qquad \times [1 - P(b)] + 2p_2 P^2(b)\} b \, db \,,\end{aligned} \tag{5}$$

$$\begin{aligned}\sigma(K) &= 2\pi(p_1 + 2p_2) \int_0^\infty P(b) b \, db \\ &= \tfrac{1}{6} R \times 2\pi \int_0^\infty P(b) b \, db \,,\end{aligned} \tag{6}$$

where b is the impact parameter and $P(b)$ is the probability of a $(2p\pi)^{-1}$ to $(2p\sigma)^{-1}$ rotationally induced transition. The three terms in the first integrand [expression (5)] are interpreted as follows: the first term gives the probability of a single $2p\pi$ vacancy which makes a transition to the $2p\sigma$ MO; the next term gives the probability of a double $2p\pi$ vacancy leading to a single $2p\sigma$ vacancy; the third term gives the probability of a double $2p\pi$ vacancy evolving into a double $2p\sigma$ hole. In each case, the total number of empty $2p\sigma$ MO's gives the total number of K-shell excitations after the collision. Briggs and Macek merely counted the total number of K-shell excitations that were produced by all three types of events.

B. Double K-shell excitations in the same atom

The $K\alpha\alpha$ two-electron, one-photon transitions and the $K\alpha hs$ hypersatellite lines are events in which both K-shell vacancies of a double excitation end on the same atom. In principle, a coincidence experiment could distinguish events in which a double K-shell excitation led to single excitation of both atoms after the collision.

The cross section for a double K-shell excitation follows immediately from the Briggs-Macek model, as outlined above. The result is

$$\sigma(2p\sigma^{-2}) = 2\pi \int_0^\infty p_2 P^2(b) b\, db$$

$$= \tfrac{2}{144}\pi R^2 \int_0^\infty P^2(b) b\, db\,. \qquad (7)$$

C. Vacancy sharing

The rotational coupling mechanism does not directly lead to two electron K excitations in a single atom upon separation. The formation of this final state is readily visualized by considering the K-shell core of the doubly excited colliding system, in which there are two electrons. There are four electronic states in this system, which are given in Table II. Two of these states, N and Z, are g (even parity) and two, T and V, are u (odd parity).

The rotational coupling mechanism initially excites the N state with two electrons remaining in the $1s\sigma$ MO. Because the Hamiltonian operator is totally symmetric, any further excitations can only couple to states of the same parity as N, and odd states are not excited. Thus, only the two even states, N and Z, need be considered. These are shown in the two-electron potential energy diagram given in Fig. 5.[17] Note that this differs from the usual one-electron correlation diagram, in that the energies of two electrons are taken into account.

The lower state N (the one directly excited in the collision) starts out in the united atom (UA) with the configuration $(2p)^{-2} = (1s)^2$, has the MO configuration $(2p\sigma)^{-2} = (1s\sigma)^2$, and makes an adiabatic transition to the separated atoms (SA) state at $R = \infty$ with one K-shell vacancy in each SA. The upper state Z, which is not excited directly in the collision, has both electrons in the UA $(2p)^2$ state, has the MO configuration $(2p\sigma)^2$, and dissociates adiabatically to the SA state with a double K-shell vacancy in one atom and the other atom with both K orbitals filled.

In the low-velocity limit, all collisions with double K-shell excitation lead via the N state to two atoms, each with one K-shell hole, and an unmodified Briggs-Macek treatment is still valid. At higher velocities, nonadiabatic transitions occur to the upper state Z (shown in Fig. 5), which has both K-shell vacancies in one of the separating atoms.

TABLE II. Electronic states of a diatomic system with two K-shell electrons.

Name of state	Configuration: United atom	Configuration: Molecular orbital	Configuration: Separated atoms
Z	$(2p)^2\ {}^1P, {}^1D$	$(2p\sigma_u)^2\ {}^1\Sigma_g^+$	$1s_A^2, 1s_B^2$
V	$(1s, 2p)^1P$	$(1s\sigma_g, 2p\sigma_u)^1\Sigma_u^+$	$1s_A 1s_B$
T	$(1s, 2p)^3P$	$(1s\sigma_g, 2p\sigma_u)^3\Sigma_u^+$	$1s_A 1s_B$
N	$(1s)^2\ {}^1S$	$(1s\sigma_g)^2\ {}^1\Sigma_g^+$	$1s_A 1s_B$

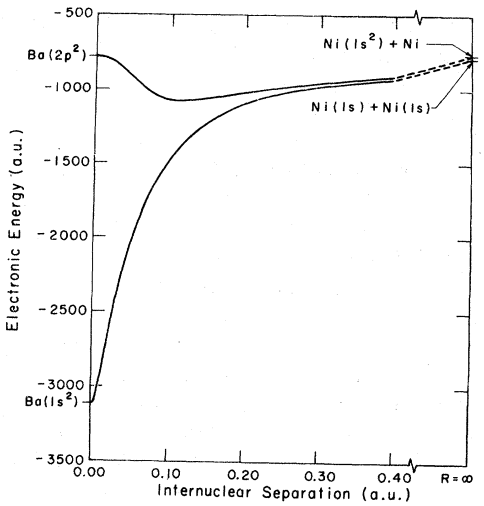

FIG. 5. Two-electron states of the core of the Ni-Ni system with a double K-shell vacancy.

The probability S of this excitation is readily calculated as a function of the projectile velocity by the Demkov-Olson-Meyerhof (DOM) formula[11]

$$S = (1 + e^{v_0/v})^{-1}\,,$$

with

$$v_0 = \pi(I_1 - I_2)/(I_1 + I_2)^{1/2}\,, \qquad (8)$$

where I_1 is the ionization potential of the lower state, I_2 the ionization potential of the upper state, and v the velocity of the incident projectile, all in atomic units. The energies of the two states at $R = \infty$ are readily calculated from simple variational theory[18] from the SA energies. They are as follows: $E(1s^2) = -(Z - \frac{5}{16})^2$, doubly occupied; and $E(1s) = -\frac{1}{2}Z^2$, singly occupied. The ionization energies are

$$I_2 = E(1s) - E(1s^2) = \tfrac{1}{2}Z^2 - \tfrac{5}{8}Z + \tfrac{25}{256}$$

and

$$I_1 = -E(1s) = \tfrac{1}{2}Z^2\,.$$

Then for the velocity v_0 in Eq. (8) we obtain

$$v_0 = \pi(\tfrac{5}{8}Z - \tfrac{25}{256})/(Z^2 - \tfrac{5}{8}Z + \tfrac{25}{256})^{1/2} \approx \tfrac{5}{8}\pi \approx 2\,,$$

where we have neglected all terms small compared to Z, which is large compared to unity. Thus, we have for the separation factor S, in expression (8),

$$S = (1 + e^{2/v})^{-1}\,, \qquad (9)$$

where it is recalled that v is in atomic units. In the present experiment of Ni on Ni collisions, the separation factor S ranges from 0.37 at 17.6 MeV to 0.44 at 91.5 MeV (see Table I).

D. Cross sections for x-ray production

The total cross section for $K\alpha$ x rays (with double vacancies counted twice) is given by Eq. (6):

$$\sigma_{K\alpha} = \omega_K \sigma(K) = \tfrac{1}{6} R \times 2\pi\omega_K \int_0^\infty bP(b)\,db\,, \qquad (10)$$

where ω_K is the fluorescent yield.

In $K\alpha hs$ hypersatellite transitions, $K\alpha$ photons are emitted from an atom with a doubly excited K shell. The cross section for these x rays is given by Eq. (7):

$$\sigma_{Khs} = \omega_{Khs} S\sigma(2p\sigma^{-2}) = \omega_{Khs} S \tfrac{1}{144} R^2 \times 2\pi \int_0^\infty bP^2(b)\,db\,, \qquad (11)$$

where ω_{Khs} is the hypersatellite fluorescent yield which may differ from ω_K. Stoller *et al.*[19] have shown that at a Ni projectile energy of 40 MeV, the cross section for $K\alpha\alpha$ photons, is smaller than that for the hypersatellite lines by a branching ratio $\eta = (5000 \pm 600)^{-1}$.

Utilizing the measured branching ratio, we obtain an expression for the cross section for the $K\alpha\alpha$ one-photon, two-electron transitions:

$$\sigma_{K\alpha\alpha} = \sigma_{Khs}\eta = \sigma(K)\tfrac{1}{24}\eta SR \left(\frac{\int_0^\infty bP^2(b)\,db}{\int_0^\infty bP(b)\,db} \right) \cdot \omega_{Khs} \qquad (12)$$

The quantity in large parentheses can be estimated as follows. The probability function $P(b)$ has been calculated by Briggs and Macek[9] and other authors.[20] In the scaled velocity range which corresponds to the present experimental conditions, the function $P(b)$ has two peaks. The first rises to a maximum of unity at very small impact parameters and contributes a negligible amount to the total cross section because of the weighting factor b in the integrand of expressions (6), (7), (10), and (11). The second peak is a broad, bell-shaped curve, with a typical maximum value of $P(b)_{\max} \approx 0.7$. For purposes of estimation, we approximate the function $P(b)$ by a normal curve

$$P(b) \approx P(b)_{\max} e^{-cx^2}\,,$$

where c is a constant and x is the deviation of the quantity b from its value at the maximum. Taking the slowly varying quantity b out of the integral leads to the following value for the quantity in large parentheses in expression (12):

$$\left(\frac{\int_0^\infty bP^2(b)\,db}{\int_0^\infty bP(b)\,db} \right) \approx \frac{P^2(b)_{\max} \int_{-\infty}^{+\infty} e^{-2cx^2} dx}{P(b)_{\max} \int_{-\infty}^{+\infty} e^{-cx^2} dx}$$

$$= P(b)_{\max} \frac{\pi/\sqrt{2c}}{\pi/\sqrt{c}} = \frac{P(b)_{\max}}{\sqrt{2}} \approx \tfrac{1}{2}\,.$$

The fact that this result is independent of energy follows from the very slow variation of $P(b)_{\max}$ with projectile energy.[20] With this estimate, double excitation cross sections become

$$\sigma_{K\alpha\alpha} = \eta\sigma_{Khs} = \sigma_{BM} \tfrac{1}{48} \eta S R^2 \omega_{Khs}, \qquad (13)$$

where $\sigma_{BM} = \sigma(K)/R$ is the Briggs-Macek cross section. As discussed below, the fluorescent yield, in general, varies with projectile energy.

E. Fluorescent yield dependence on L-shell vacancies

Owing to the molecular nature of atomic collisions, inner-shell vacancies are generally accompanied by multiple vacancies in outer shells.[13,14] The number of vacancies in outer shells can be estimated by the slight shift in the x-ray or Auger electron energies. An important effect of outer-shell vacancies is to change the fluorescent yield. This influence of outer-shell ionization on fluorescent yield has been predicted[21,22] and observed experimentally by many groups.[15,23-26]

Estimates of the effect of outer-shell vacancies involve statistical averages of calculations of fluorescent yields for individual multiplet states. Rather than perform these laborious calculations, a simplified method is presented here. We follow McGuire[27] and Larkins.[21]

The fluorescent yield ω is the ratio of radiative transition rate R_F to the sum of the radiative and Auger decay rate R_A:

$$\omega = R_F/(R_A + R_F). \qquad (14)$$

TABLE III. Comparison of approximate and exact expressions for fluorescent yields for Ne K-shell x rays.

Number of L-shell vacancies i	Fluorescent yield	
	Approximate [a]	Exact [b]
0	0.0159	0.0159
1	0.0185	0.0176
2	0.022	0.0199
3	0.0275	0.0245
4	0.036	0.039
5	0.053	0.086
6	0.101	0.229

[a] Expression (17).
[b] Reference 25.

TABLE IV. Calculation of fluorescent yields.

Projectile energy (MeV)	17.9	37.1	64.8	91.5	0[a]
$K\alpha$ x rays					
Photon energy (keV)	7.525	7.549	7.576	7.593	7.472[b]
Number of L-shell vacancies[c]	1.6	2.3	3.1	3.6	...
Fluorescent yield $\omega_{K\alpha}$[d]	0.47	0.51	0.55	0.58	0.41
$K\alpha hs$ x rays					
$K\alpha\alpha$ photon energy (keV)	15.194	15.278	15.312	15.359	15.111[c]
Number of L-shell vacancies i[c]	0.9	1.9	2.2	2.8	...
Fluorescent yield $\omega_{K\alpha hs}$[d]	0.44	0.49	0.50	0.53	0.41[e]

[a] Data in this column are for x rays in which there are no outer-shell vacancies.
[b] Source: A. E. Sandström, Handb. Phys. 30, 78 (1957).
[c] Estimation based on calculations in Ref. 7.
[d] Calculated from expression (17).
[e] Per K-shell vacancy.

The radiative decay rate is a one-electron process and is proportional to the number of L-shell electrons[21] N_L:

$$R_F = R_{F0}(\tfrac{1}{8}N_L), \tag{15}$$

where R_{F0} is the corresponding decay rate for a completely filled L shell.

The Auger decay rate is a two-electron process and therefore depends statistically on the number of combinations of two out of N_L electrons[27]:

$$R_A = R_{A0}(N_L)(N_L - 1)/8 \times 7, \tag{16}$$

where R_{A0} is the corresponding decay rate for a completely filled L shell. With the substitution of the vacancy number $i = 8 - N_L$ into these expressions, the fluorescent yield ω in expression (14) becomes

$$\omega = \omega_0/[1 - \tfrac{1}{7}i(1 - \omega_0)], \tag{17}$$

where ω_0 is the fluorescent yield for a completely filled L shell ($\omega_0 = 0.41$ for Ni). The latter is obtained from x-ray yields resulting from photon-, electron-, or proton-induced x rays.

Table III compares fluorescent yields from expression (17) with the more exactly calculated values of Chen *et al.*[25] for neon atoms in various states of ionization. The yields agree within about 10% up to four vacancies and diverge beyond this value. Since the maximum number of vacancies is less than four in the present experiment (see Table IV), we have employed this simplified model.

Table IV contains details of calculation of fluorescent yields for the present experiment. The number of L-shell vacancies is obtained from the photon energy and the theoretical energy shift per L-shell vacancy.[7] Mean values of L-shell vacancies used for calculating the $K\alpha$ fluorescent yields are taken from energy shifts of the $K\alpha$ line. Values used in calculating the hypersatellite fluorescent yield are taken from energy shifts of the $K\alpha\alpha$ two-electron, one-photon transition line as calculated in Ref. 7.

IV. APPLICATION TO EXPERIMENTAL RESULTS

As discussed in Sec. III, the measurements presented here were conducted within a projectile velocity range ($0.12 \leq v/v_B \leq 0.26$) in which dynamically induced vacancies play an important role in the excitation mechanism. We have already noted that with measurements of both single and double K-shell excitations available, it becomes possible to test both the Briggs-Macek calculation[9] and the vacancy production mechanisms postulated by Fastrup *et al.*[10]

A. Relative cross sections

Within the framework of the Briggs-Macek theory, the number of double K-shell vacancies should be proportional to the *square* of the vacancy factor R. Thus a simple test of the theory can be made. In Fig. 3 are plotted both the ratios of the $K\alpha$ excitation cross section to the theoretical value (see also Table I), and the ratios of the $K\alpha\alpha$ to $K\alpha$ cross sections. By the arguments presented above, both should be proportional to R. Both follow approximately a relationship of the form $R = \text{const} \times e^{-a/v}$, with values for a that deviate by 15% while the rms experimental error on the comparison is ~8%.

B. Absolute cross sections

The results in Sec. III D are absolute. The vacancy factor R is determined from the single excitation cross section $\sigma_{K\alpha}$ and is used to calculate the

absolute cross section for the two-electron, one-photon cross section $\sigma_{K\alpha\alpha}$ with no further adjustment of parameters.

Table I gives the values of all the quantities that enter into the calculation and compares the calculated and measured $K\alpha\alpha$ cross sections, which also are shown in Fig. 2. Considering that the absolute experimental cross sections are uncertain due to a target thickness measurement error of ~±20%, the agreement of theory with experiment is very good.

C. Scaling behavior of the velocity dependence of the vacancy factor R

A further test of the experimental results is the velocity dependence of the vacancy factor R, which is shown in Fig. 3. The constant a in the expression $R = \text{const} \times e^{-a/v}$ has the dimensions of a velocity, which should scale as the atomic number Z of the collision partners. It is of interest to compare the present result with that of Stolterfoht *et al.*,[15] who found $a = 1.85$ for K-shell excitation of Ne by Ne^0 atoms, 3.0 for Ne^+ on Ne, and 3.4 for Ne^{++} on Ne. If one scales the present value for $a = 9.1 \pm 0.4$ for Ni on Ni, by the ratio of atomic numbers, the result is

$$a_{Ne} = a_{Ni} Z_{Ne}/Z_{Ni} = (9.1 \pm 0.4)/2.8 = 3.25 \pm 0.14.$$

The results are in excellent agreement with those of Stolterfoht *et al.* for Ne^{++} and Ne^+, although neither set of results agrees with those for neutral neon.

Cocke *et al.*[28] have measured the impact parameter dependence for production of single Cl and Ar K vacancies in the bombardment of argon-gas targets by chlorine projectiles. These authors found $a = 11$, which when scaled to Ni on Ni, would become $a = 2.8/17.5 \times 11 = 17.6$, in disagreement with the present results. The reason for the disagreement presumably lies in the difference between the two experiments in the condition of the outer shells prior to the collision. In the present experiment, after the projectiles reach charge equilibrium in the foil, the incident Ni ions are stripped of essentially all the 18 outer M-shell electrons.[29] In the experiment of Stolterfoht *et al.*,[15] there are no M-shell electrons. Thus, both experiments are comparable and the results agree. In the experiment of Cocke *et al.*,[28] the M shell is filled prior to the gas-phase collision. Thus $2p\pi$ vacancies must be created in a single collision by M-shell excitation [process (c) in Fig. 4], followed by L-M transitions [process (b) in Fig. 4], or direct transitions from the L shell to highly excited or continuum orbitals. For either process, it is reasonable to assume a larger value of the exponential factor a.

V. DISCUSSION: ELECTRON PROMOTION MODEL

The comparison of relative cross sections, shown in Fig. 3 and discussed in Sec. IV A, is the most sensitive comparison of theory and experiment, since many absolute errors in measurement and theory are absent.

The small (15%) difference between relative cross sections, which is on the margin of experimental errors, could be due to a variation of the branching ratio $\eta = \sigma_{K\alpha\alpha}/\sigma_{Khs}$ over the projectile energy range of the experiment.

The reasonable agreement between calculated and measured relative cross sections verifies that the electron promotion model[13,14] and the exit channels mechanism[10] provide an essentially correct description of the inner-shell vacancy production for the conditions of the present experiment. In particular, the velocity dependence predicted by the Briggs-Macek calculation[9] is verified. Clearly, the relative cross sections do not test the absolute values of the theoretical cross sections, nor test the absolute value of the vacancy factor R.

The agreement of absolute cross sections, as shown in Fig. 2, confirms those aspects of the Briggs-Macek calculation not tested by the comparison of relative cross sections. Moreover, the agreement of the scaled velocity dependence of the vacancy factor is further confirmation of the Briggs-Macek model,[9] as modified by Fastrup *et al.*[10] to take into account velocity-dependent vacancy factors.

The experimental results obtained by Stolterfoht *et al.*[15] were from collisions with Ne atoms in the gas phase. These necessarily were single-collision processes, in which the L-shell, exit channel vacancies were produced in the same, single collision as the K-shell excitation. The agreement of our scaled velocity dependence with the Ne results is consistent with the single-collision process. Other workers have found a two-collision process in K-shell excitation in collision with solid targets, where L-shell vacancies were created in prior collisions.[16] Only if the velocity dependence for such a process fortuitously agreed with the single-collision mechanism, could our results be explained by the "solid effect."[16]

Nevertheless, the discrepancy of a factor of 4 between our results and the thin-target experiments of Kubo *et al.*[30] suggest that a solid effect may exist. Similar foil thickness effects have been found by many groups.[31-35] The effect is subtle. In our case, prior collisions create M-shell vacancies, as discussed in Sec. IV C. These enhance the K-shell cross sections indirectly by opening exit channels for velocity-dependent ex-

citation out of the $2p\pi$ MO. These excitations in turn provide exit channels for the $2p\sigma$-$2p\pi$ rotational coupling, which leads to K-shell excitation.

In general, excitation in solids, according to the electron promotion model[13,14] is like peeling an onion. Excitation starts in outer shells and works its way into inner shells through successive processes. In some cases, as in the present, two or more of these excitations can occur in the same collision.

It is also clear from the absolute results that, under the present experimental conditions, non-electron-promotion processes, such as direct excitation of $1s\sigma$ or $2p\sigma$ electrons into the continuum or high MO's [processes (d) and (e) in Fig. 4] are at most of the order of the experimental error of 20% of the total cross section.[36]

One example of such excitation is known from Bayfield's work on $2s$ excitation in proton-hydrogen collisions.[37] This cross section first becomes observable in his experiments at 4 keV, at a velocity equal to $0.4\ V_B$, far above that of the present experiment ($v \leq 0.26\ V_B$). A scaled value of his cross section is 600 b at 260-MeV Ni on Ni and is certainly negligible in the energy range under consideration, in agreement with the present results.

Recently Schuch *et al.*[38] have reported a strong impact parameter dependence of the $K\alpha\alpha$ emission probability in 35-MeV Cl-Cl collisions. These results occurred at values of $b \approx 100$ fm. Schuch *et al.*[38] interpreted these results to indicate a "new ionization mechanism," possibly direct excitation out of the $1s\sigma_g$ MO. Again, the total cross section for such events is very small and has no bearing on the interpretation of the present experiment.

Although our results for single $K\alpha$ x-ray cross sections agree in absolute magnitude with those of Laubert *et al.*[39] at lower energies, the slopes of the two sets of cross sections disagree. Since both experiments were done with the same foil thicknesses, the disagreement may arise from the different procedures employed for normalizing the accumulated beam and making finite target thickness corrections.

Within the framework of molecular-orbital theory, two-electron interactions generally are very small, except during the transition into separated atoms. The separation factor arising from this process is large (see Table I) but is calculable from the Demkov-Olson-Meyerhof equation. This part of the excitation process seems satisfactorily accounted for.

Finally, it should be noted that although the empirical procedures of Fastrup *et al.*[10] account for the vacancy factor R, there are no calculations which reveal the dynamic origin of the exit channels. At present, the route by which these channels are opened remains unknown.

VI. SUMMARY

The agreement between theory and experimental results is generally good and can be taken as a confirmation of the Briggs-Macek picture of K-shell excitation, within the framework of the electron promotion model. The dynamically induced exit channel factors, introduced by Fastrup *et al.*, have been checked independently for the first time, and also are found to scale with atomic number, as would be expected. However the origin of the dynamical production of these exit channel vacancies is as yet unknown and represents an unsolved problem for atomic collision theory.

ACKNOWLEDGMENTS

We should like to thank J. Tanis and B. Hodge for helpful discussions.

*Work supported under USERDA Contract No. E(11-1)-3074 and NSF Grant No. PHY74-09408A02.

†A preliminary report of these results was presented at the International Conference on the Physics of X-ray Spectra, August 30–September 2, 1976, National Bureau of Standards, Gaithersburg, Md., Program and Extended Abstracts, p. 180.

[1]W. Wölfli, Ch. Stoller, G. Bonani, M. Suter, and M. Stockli, Phys. Rev. Lett. 35, 656 (1975).

[2]Th. P. Hooghamer, P. Woerlee, F. W. Saris, and M. Gavrila, Second International Conference on Inner-Shell Ionization Phenomena, Freiburg, March 29–April 2, 1976 (unpublished).

[3]R. Schuch, H. Schmidt-Bocking, R. Schulé, G. Nolte, I. Tserruya, W. Lichtenberg, and K. Stiebing, Second International Conference on Inner-Shell Ionization Phenomena, Freiburg, March 29–April 2, 1976 (unpublished).

[4]W. W. Jacobs, B. L. Doyle, S. M. Shafroth, and J. A. Tanis, Bull. Am. Phys. Soc. 21, 649 (1976).

[5]A. R. Knudson, R. W. Hill, P. G. Burkhalter, and D. J. Nagel, Bull. Am. Phys. Soc. 21, 649 (1976).

[6]S. D. Dow and D. R. Franceschetti, Phys. Lett. A 50, 1 (1974).

[7]W. L. Luken, J. S. Greenberg, and P. Vincent, Phys. Rev. A 15, 2305 (1977). See also H. P. Kelly, Phys. Rev. Lett. 37, 386 (1976); also W. Hodge, Ph.D. thesis (U. of Texas, 1976) (unpublished).

[8]T. Åberg, K. A. Jamison, and P. Richard, Phys. Rev. Lett. 37, 63 (1976).

[9]J. H. Macek and J. S. Briggs, J. Phys. B 5, 579 (1972); 6, 841 (1973); 6, 982 (1973).

[10]B. Fastrup, E. Bøving, G. A. Larsen, and P. Dahl, J. Phys. B 7, L206 (1974).

[11]W. E. Meyerhof, Phys. Rev. Lett. 31, 1341 (1973). Two alternative expressions sometimes appear in the

literature for this formula: $v_0 = \pi(I_1 - I_2)/\sqrt{2}(I_1^{1/2} + I_2^{1/2})$, and $v_0 = \sqrt{2}\pi(I_1^{1/2} - I_2^{1/2})$. All three expressions are equivalent for small values of the difference $I_1 - I_2$.

[12]W. Wölfli and H. D. Betz, Phys. Rev. Lett. 37, 61 (1976).

[13]U. Fano and W. Lichten, Phys. Rev. Lett. 14, 627 (1965).

[14]W. Lichten, Phys. Rev. 164, 131 (1967); M. Barat and W. Lichten, Phys. Rev. A 6, 211 (1972).

[15]N. Stolterfoht, D. Schneider, D. Burch, B. Aagaard, E. Bøving, and B. Fastrup, Phys. Rev. A 12, 1313 (1975).

[16]F. W. Saris, W. F. van der Weg, H. Tawara, and R. Laubert, Phys. Rev. Lett. 28, 717 (1972); F. W. Saris, in *Seventh ICPEAC, Invited Talks and Progress Reports*, edited by T. R. Govers and F. J. deHeer (North-Holland, Amsterdam, 1971).

[17]We are indebted to Neil Ostrove for calculations, construction of Fig. 4, and for pointing out to us expression (9).

[18]See, for example, H. A. Bethe and R. Jackiw, *Intermediate Quantum Mechanics*, 2nd ed. (Benjamin, Reading, Mass., 1968), p. 42.

[19]Ch. Stoller, W. Wölfli, G. Bonani, M. Stöckli, and M. Suter, Phys. Lett. A 58, 18 (1976).

[20]See, for example, D. R. Bates and D. A. Williams, Proc. Phys. Soc. Lond. 83, 425 (1964), Fig. 2.

[21]F. P. Larkins, J. Phys. B 4, L29 (1971); 4, 14 (1971).

[22]D. Burch, W. B. Ingalls, J. S. Risley, and R. Heffner, Phys. Rev. Lett. 29, 1719 (1972).

[23]D. Burch, N. Stolterfoht, D. Schneider, H. Wieman, and J. S. Risley, Phys. Rev. Lett. 32, 1151 (1974).

[24]C. P. Bhalla, D. L. Mathews, and C. F. Moore, Phys. Lett. A 46, 336 (1973); C. P. Bhalla, *ibid.* 46, 185 (1973).

[25]M. H. Chen, B. Crasemann, and D. L. Mathews, Phys. Rev. Lett. 34, 1309 (1975).

[26]R. L. Kauffman, K. A. Jamison, T. J. Gray, and P. Richard, Phys. Rev. Lett. 36, 1074 (1976).

[27]E. J. McGuire, Phys. Rev. 185, 1 (1969).

[28]C. L. Cocke, R. R. Randall, S. L. Varghese, and B. Cornutte, Phys. Rev. A 14, 2026 (1976).

[29]H. D. Betz, Rev. Mod. Phys. 44, 465 (1974), see Eq. (5.8) and Fig. 5.10, which were originally derived by V. S. Nikolaev and I. S. Dmitriev, Phys. Lett. A 28, 277 (1968). The Nikolaev-Dmitriev formula gives 15–22 electrons stripped over the energy range of our experiment. The actual number is probably slightly smaller within the solid foil.

[30]H. Kubo, F. C. Jundt, and K. H. Purser, Phys. Rev. Lett. 31, 674 (1973).

[31]W. Brandt, R. Laubert, M. Mourino, and A. Schwarzschild, Phys. Rev. Lett. 30, 358 (1973).

[32]F. Hopkins, Phys. Rev. Lett. 35, 270 (1975).

[33]K. O. Groeneveld, B. Kolb, J. Schader, and K. D. Sevier, Z. Phys. A 277, 13 (1976).

[34]L. C. Feldman, P. J. Silvermann, and R. J. Fortner, Nucl. Instrum. Methods 132, 29 (1976).

[35]H. D. Betz, F. Bell, H. Panke, G. Kalkoffen, M. Welz, and D. Evers, Phys. Rev. Lett. 33, 807 (1974).

[36]For discussions of these mechanisms (shown in Fig. 4), see W. E. Meyerhof, Phys. Rev. A 10, 1005 (1974); W. E. Meyerhof, R. Anholt, T. K. Saylor, S. M. Lazarus, A. Little, and L. F. Chase, Jr., *ibid.* 14, 1653 (1976); J. H. McGuire and P. Richard, *ibid.* 8, 1374 (1973); C. Foster, T. P. Hoogkamer, P. Woerlee, and F. W. Saris, J. Phys. B 9, 1943 (1976).

[37]J. E. Bayfield, Phys. Rev. 185, 105 (1969); J. E. Bayfield, Phys. Rev. Lett. 25, 1 (1970).

[38]R. Schuch, G. Nolte, H. Schmidt-Böcking, R. Schulé, W. Lichtenburg, R. E. Stiebing, and I. Tserruya, International Conference on the Physics of X-ray Spectra, National Bureau of Standards, Gaithersburg, Md., Aug. 30–Sept. 2, 1976 (unpublished).

[39]R. Laubert, H. Haselton, J. R. Mowat, R. S. Peterson, and I. A. Sellin, Phys. Rev. A 11, 135 (1975).